

Atomistic studies of interactions between the dominant lattice dislocations and γ/γ -lamellar boundaries in lamellar γ -TiAl

I.H. Katzarov*, A.T. Paxton

Atomistic Simulation Centre, School of Mathematics and Physics, Queen's University Belfast, Belfast BT7 1NN, Northern Ireland, UK

Received 17 December 2008; received in revised form 26 March 2009; accepted 30 March 2009

Available online 4 May 2009

Abstract

This paper reports on atomistic simulations of the interactions between the dominant lattice dislocations in γ -TiAl (ordinary screw $\frac{1}{2}\langle 110 \rangle$ and $\langle 101 \rangle$ superdislocations) with all three kinds of γ/γ -lamellar boundaries in polysynthetically twinned (PST) TiAl. The purpose of this study is to clarify the early stage of lamellar boundary controlled plastic deformation in PST TiAl. The interatomic interactions in our simulations are described by a bond order potential for L1₀-TiAl which provides a proper quantum mechanical description of the bonding. We are interested in the dislocation core geometries that the lattice produces in proximity to lamellar boundaries and the way in which these cores are affected by the elastic and atomistic effects of dislocation-lamellar boundary interaction. We study the way in which the interfaces affect the activation of ordinary dislocation and superdislocation slip inside the γ -lamellae and transfer of plastic deformation across lamellar boundaries. We find three new phenomena in the atomic-scale plasticity of PST TiAl, particularly due to elastic and atomic mismatch associated with the 60° and 120° γ/γ -interfaces: (i) two new roles of the γ/γ -interfaces, i.e. decomposition of superdislocations within 120° and 60° interfaces and subsequent detachment of a single ordinary dislocation and (ii) blocking of ordinary dislocations by 60° and 120° interfaces resulting in the emission of a twinning dislocation.

© 2009 Acta Materialia Inc. Published by Elsevier Ltd. All rights reserved.

Keywords: Atomistic simulation; Titanium alloys; Dislocations; Interfaces; Plastic deformation

1. Introduction

The physical and mechanical properties of γ -based titanium aluminide alloys, such as their low density, high thermal conductivity and high-temperature strength, make these materials attractive candidates for high-temperature weight-critical applications [1,2]. Only the γ -TiAl (tetragonal L1₀) and α_2 -Ti₃Al (hexagonal DO₁₉) phases have mechanical properties that are suitable for industrial applications. In spite of their promising high-temperature properties the α_2 and γ single-phase components are both quite brittle and hence have not attracted much industrial interest. Acceptable combinations of strength, ductility and toughness can be achieved by special heat treatments

leading to the formation of a two-phase lamellar microstructure consisting of layers of α_2 -Ti₃Al, the minority phase and γ -TiAl, the majority phase. Surprisingly, the lamellar character leads to useable room temperature ductility, which is very low in monolithic TiAl [1–3].

The improvement in mechanical properties is presumably due to the presence of lamellar boundaries in the material. There are three types of γ/γ -interfaces formed by rotation about the [111] axis at angles of 60°, 120° and 180° [4]. A similar orientation-based classification exists also for γ/α_2 -interfaces. It is well understood that the mechanical properties are primarily controlled by the γ/γ -interfaces, as they are much more frequent than those of the γ/α_2 -type, but there is as yet a lack of detailed understanding of the mechanical behaviour of lamellar γ -TiAl [2,4]. The main deformation modes in γ -TiAl are slip and twinning, both of which operate on one of the close-packed {111} planes [5]. Slip occurs via two types of dislocations:

* Corresponding author.

E-mail address: i.katzarov@qub.ac.uk (I.H. Katzarov).

ordinary dislocations with Burgers vector $\frac{1}{2}\langle 110 \rangle$ and $\langle 101 \rangle$ superdislocations. The observed twinning elements are $K_1 = (111)$ and $\eta_2 = [\bar{1}12]$ [6]. It is worthwhile to remember in what follows that $\frac{1}{6}\langle 112 \rangle$ dislocations are “twinning” and trail a superlattice intrinsic stacking fault (SISF), while $\frac{1}{6}\langle 211 \rangle$ dislocations are “pseudotwinning” and trail a complex stacking fault (CSF) [7]. In single γ crystals, superdislocations dominate at low temperatures and the glide of ordinary dislocations and twinning become significant only at high temperatures [5,8]. By contrast, transmission electron microscopy (TEM) studies showed that the γ phase in the two-phase material deforms mostly by ordinary dislocation slip and twinning at room temperature. The glide of $\langle 101 \rangle$ superdislocations becomes significant only at high temperatures [4]. The reasons behind this phenomenon are poorly understood.

When a polycrystalline metal undergoes plastic deformation, a large number of lattice dislocations impinge on lamellar boundaries and interact with them. The lamellar interfaces are found to play dual roles. One is to serve as major sources of dislocations and the other is to impede the movement of the dislocations and twins [2,4]. We now find two further roles, as we report below and discuss in Section 4. Investigating the function of the lamellar structure is key to understanding the deformation mechanisms of the material and guiding future material design to improve properties. To understand the role the lamellar boundaries play in enhancing the ductility, and the difference between deformation mechanisms in single-phase and two-phase TiAl alloys, we have to gain deeper insight into the mechanisms of deformation and the transmission of dislocations across the lamellar boundaries at the atomic scale.

Detailed behaviour of dislocations, structures of lamellar boundaries and their mutual interactions at the atomic level can be extremely complex and the only plausible way of studying such phenomena is by means of computer simulation. Since the mechanisms of the interactions between dislocation cores and lamellar boundaries are of fundamental significance for understanding of the early stage of lamellar boundary controlled plastic deformation, the present study is focused on investigation of the dislocation-lamellar boundary interactions in γ -TiAl by means of atomistic simulations. While simulations of individual dislocations and grain boundaries are commonly carried out even with highly accurate first-principles methods, simulations of the interactions between two defects are still quite rare. The reason is the great complexity of the problem, which requires extensive simulation blocks, careful handling of boundary conditions and reliable models of interatomic interactions. The interaction mechanisms in various face-centred cubic (fcc) metals [9–11] and transfer of slip at interfaces between different materials [12–14] have been studied recently by several groups. The atomic mechanisms responsible for the emission of partial dislocations from grain boundaries in nanocrystalline metals

have been studied in several simulations [15–17]. In Ref. [18] we performed atomistic simulation of the core structure and glide of ordinary $\frac{1}{2}\langle 110 \rangle$ screw dislocations in two γ lamellae forming a 180° twin γ/γ -interface using recently constructed bond order potentials (BOPs) [19,20]. We studied dislocation glide along a twin interface, transmission of an ordinary screw dislocation between lamellae, and the core structure, mobility and detachment of an interfacial $\frac{1}{2}\langle 110 \rangle$ screw dislocation from a twin boundary under applied shear stresses in directions parallel and perpendicular to a (111) plane.

In this work we present results of atomistic simulations of the interactions between the dominant lattice dislocations in γ -TiAl (ordinary screw $\frac{1}{2}\langle 110 \rangle$ and $\langle 101 \rangle$ superdislocations) with the all three kinds of γ/γ -lamellar boundaries in lamellar TiAl. In our simulations, we have used the BOP for TiAl developed in Refs. [20,21]. We are interested in the dislocation core geometries that the lattice produces in proximity to lamellar boundaries and the way in which these cores are affected by the elastic and atomistic effects of dislocation-lamellar boundary interaction. We study the way in which the interfaces affect the activation of ordinary dislocation and superdislocation slip inside the γ lamellae and transfer of plastic deformation across lamellar boundaries. Based on the results of these calculations we suggest reasons for the difference between deformation mechanisms in single-phase and lamellar TiAl alloys.

2. Simulation methodology

The most important precursor of atomistic simulations involving systems composed of a large number of atoms is a reliable description of interatomic interactions. First-principles methods based on density functional theory (DFT) provide such a description most reliably but are limited by feasible block sizes that contain not more than a couple of hundred atoms and usually require use of periodic boundary conditions that are not well suited for dislocation studies. While isolated dislocations and grain boundaries can be treated nowadays with great accuracy by DFT methods, simulations of mutual interactions between dislocations and grain boundaries are still beyond the reach of these methods because of computational demands. In order to describe processes of such complexity one has to cross the bridge between the electronic-structure calculations and atomistic simulations by coarse-graining the electronic degrees of freedom into many-body interatomic potentials.

BOPs were first formulated by Pettifor and co-workers [19,22–24] and represent a numerically efficient scheme that expresses the orthogonal tight-binding approximation in terms of short-range non-central interatomic potentials. The multi-atom character of the forces is thereby captured in a physical way that goes beyond the standard pair functionals (Finnis–Sinclair, embedded atom method), and BOPs can describe features such as the negative Cauchy

pressures ($C_{13} - C_{44} < 0$, $C_{12} - C_{66} < 0$) that simpler models cannot. Apart from their genuine quantum-mechanical origin, BOPs have two additional important advantages. First, the evaluation of the energy scales linearly in computational time with the number of atoms, and, second, the real-space formalism avoids the need to impose full periodic boundary conditions common to k-space methods. Both of these features are crucial for studies of dislocations since such simulations often require a large number of atoms and complex geometries.

Recently, a BOP for γ -TiAl was constructed and extensively tested against accurate first-principles methods in order to assess the potential's reliability and applicability [20,21]. For dislocation studies, the most important factors are the energies of stacking-fault-like defects, whose values calculated from the BOP agree well with those found by DFT-based calculations [25–27]. Atomistic simulations of the core structure and glide of the ordinary screw $\frac{1}{2}\langle 110 \rangle$ dislocation and the screw $\langle 101 \rangle$ superdislocation in single-phase L₁₀-TiAl have been performed using the BOP [28,29], which has also been used for atomistic simulations of the core structure and glide of ordinary $\frac{1}{2}\langle 110 \rangle$ screw dislocations in two L₁₀-TiAl lamellae forming a 180° twin γ/γ -interface [18].

Rectangular parallelepiped simulation cells were used in the present simulations of dislocation-lamellar boundary interactions. The γ/γ interfaces were created by rotation of the upper half of the block with respect to the lower by 60°, 120° and 180° about the [111] direction (the y-axis of the simulation cell is set parallel to the [111] direction). Orientation relations are: in the 60° interface [110][101]; and in the 120° interface [110][011]. The L₁₀-TiAl crystal containing a γ/γ interface was constructed from four successive planes forming one period in these parallel directions, along which periodic boundary conditions were applied. We set the z-axis of the simulation cell parallel to the above parallel directions of two adjacent gamma lamellae. The x-axis is set parallel to the lamellar boundaries.

The atomistic calculations of dislocation-180° γ/γ -interface interactions were carried out using the BOP for TiAl developed in Ref. [20], which is fitted to reproduce the correct lattice parameters. Due to the non-ideal c/a ratio ($c/a = 1.016$), the 60° and 120° interfaces, where the two non-equivalent directions [110] and [101] overlap, will have regions of misfit. A network of misfit dislocations compensates for the misfit in these cases. The deviation from non-ideality is very small and therefore misfit dislocations will be about 60 lattice spacings apart with large coherent regions in between them [30]. In order to avoid the slight mismatch between the two lattices, and thus use of very large repeat cells, we used a modified BOP for TiAl [20,21] for simulation of 60° and 120° interfaces. The modified BOP for TiAl makes the L₁₀ structure stable for $c/a = 1.0$ rather than 1.016. In our calculations we effectively study the structure of the regions of matching lattices between the misfit dislocations.

3. Results

3.1. Modelling of interactions between a screw $\frac{1}{2}\langle 110 \rangle$ dislocation and 60° and 120° γ/γ -interfaces

3.1.1. Static core structure

Atomistic simulations of the structure and properties of ordinary $\frac{1}{2}\langle 110 \rangle$ screw dislocations in single-crystal L₁₀-TiAl using the BOP for γ -TiAl [18,28] suggest, similarly to the results of ab initio calculations [25], that the ordinary screw dislocation in the γ -phase material possesses a non-planar core, spread symmetrically into two planes of the (111) type. In principle, a planar configuration corresponding to the dissociation into Shockley partials separated by the CSF could exist. However, the non-planar core is the only structure found. The reason is, apparently, the high energy of the CSF (412 mJ m⁻²) in L₁₀-TiAl. Atomistic simulations of interactions between a $\frac{1}{2}\langle 110 \rangle$ dislocation and the 180° twin γ/γ -interface in lamellar TiAl indicate that the ordinary dislocation retains its non-planar sessile core structure in proximity to the 180° lamellar boundaries [18].

In order to study the core structure and to test stability of an ordinary screw dislocation at 60° and 120° lamellar boundaries we introduced the initial centre of the elastic field of a perfect dislocation in the vicinity of the lamellar boundary. The resulting relaxed core structures are shown in Fig. 1. Close to the 60° and 120° lamellar interfaces the $\frac{1}{2}\langle 110 \rangle$ screw dislocation is attracted to the interface where it splits into two Shockley partials separated by CSF according to the reaction:

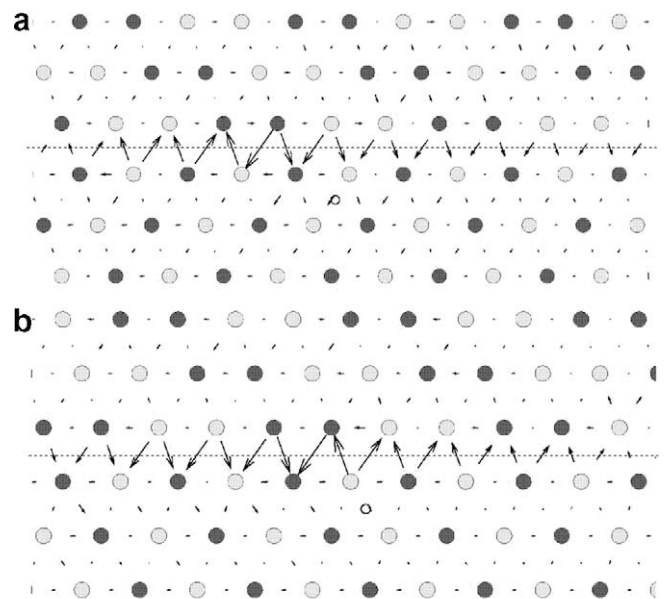
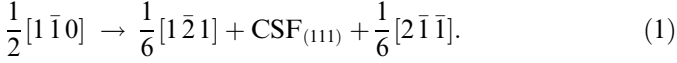


Fig. 1. Differential displacement maps of the planar splitting of $\frac{1}{2}\langle 110 \rangle$ screw ordinary dislocation at (a) the 120° and (b) the 60° γ/γ -lamellar boundaries. All atomic displacements are normal to the plane of the paper; the lengths of arrows describe the amount of relative displacement of pairs of atoms [42]. The open circle marks the elastic centre of the dislocation.



These dissociations take place because the energy of the CSF at the 120° and 60° lamellar boundaries predicted by BOP in agreement with ab initio calculations (260 mJ m⁻² at 60° and 270 mJ m⁻² at 120°) [31] is considerably smaller than the energy of the CSF in bulk TiAl. On the other hand, the CSF energy is higher when the fault lies in the 180° interface (see Section 3.2.2.2).

3.1.2. Effects of applied stress

3.1.2.1. Stress generating glide force parallel to the lamellar boundaries. In order to study the glide of the planar core configurations under the effect of externally applied shear stress we started with simulation blocks containing the fully relaxed planar core structure of an interfacial $\frac{1}{2}[1\bar{1}0]$ screw dislocation (Fig. 1). The shear stress was applied in the $\frac{1}{2}[1\bar{1}0]$ direction in such a way that the dislocation was set to glide on the lamellar boundary plane. In practice, this stress is imposed by applying the appropriate homogeneous shear strain, which is evaluated with anisotropic elasticity theory. The shear strain was gradually increased in small increments and the block fully relaxed after each step.

When applying the shear stress such that the $\frac{1}{6}[2\bar{1}\bar{1}]$ partial bounding the CSF would be leading during glide, the dislocations start to move under an applied stress of 0.015C₄₄. If the stress in the (111) plane acts such that the $\frac{1}{6}[1\bar{2}1]$ dislocation of reaction (1) would be leading, the planar configuration starts to move at considerably lower stress, namely 0.002C₄₄. The results of the present simulations indicate that the dissociated planar core of $\frac{1}{2}[1\bar{1}0]$ ordinary dislocation in the 60° and 120° lamellar boundaries is glissile and starts to move along the interfaces at considerably lower applied stress than the non-planar sessile core structure of $\frac{1}{2}[1\bar{1}0]$ screw dislocation in single-crystal L1₀-TiAl. Interestingly, the Peierls stress for ordinary dislocation glide in 60° and 120° lamellar boundaries plane is therefore smaller than the critical resolved shear stress (CRSS) for activation of the dominant slip mode in L1₀-TiAl {101} superdislocation glide [28,29].

3.1.2.2. Stress generating glide force perpendicular to the lamellar boundaries. Under applied shear stress generating glide force perpendicular to the lamellar boundary in the direction of the second lamella, the core of the dissociated $\frac{1}{2}[1\bar{1}0]$ screw dislocation transforms to a non-planar sessile structure spreading onto the lamellar interface and an intersecting (111) plane in the second lamella (Fig. 2). The analysis of the core structures reveals that they correspond to dissociation into three partial dislocations (one of them locked at the interface) separated by a CSF and SISF in the (111) plane according to the reactions:

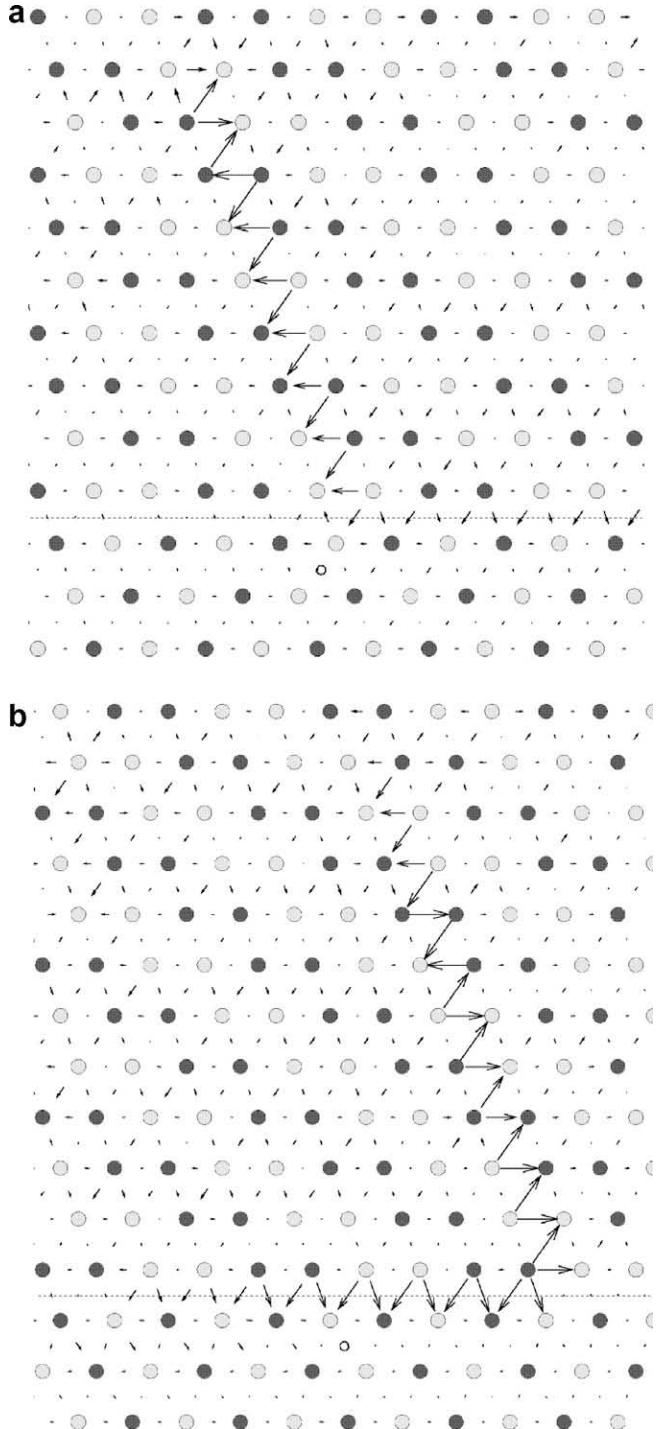
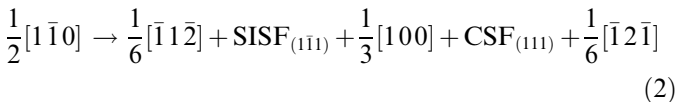
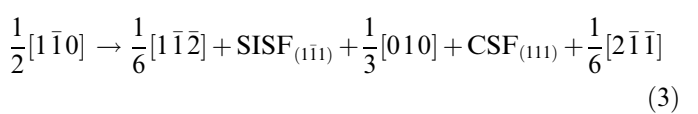


Fig. 2. Effect of applied shear stress inducing glide force in direction perpendicular to the lamellar boundaries on the planar splitting $\frac{1}{2}<110>$ screw ordinary dislocation at (a) the 120° and (b) the 60° γ/γ -interfaces.

for the 120° lamellar boundary, and:



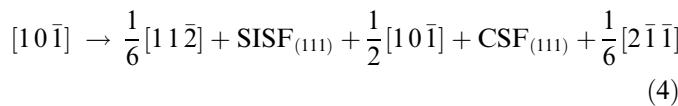
for the 60° lamellar boundary. We use Burgers vector notations according to the coordinate system of the first lamellae for the left-hand side of the reactions and coordi-

nate system of the second crystal for the right-hand side. Ribbons of SISF are formed in the second lamellae as result of propagation of $\frac{1}{6}\langle 112 \rangle$ twinning partial dislocations into the $(\bar{1}\bar{1}1)$ plane. The width of the SISF increases with increase of the applied shear stress.

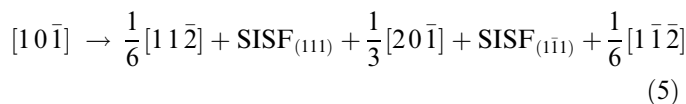
When stress is applied in the reverse direction (the glide force acts to drive the dislocation towards the first lamella), the planar core configuration gradually constricts with increasing stress (Fig. 3a). Under an applied stress of $0.035C_{44}$ the interfacial planar configuration detaches from the lamellar boundary and transforms into a lattice $\frac{1}{2}\langle 1\bar{1}0 \rangle$ screw dislocation in the first lamella (Fig. 3b). The effect of further stress on the configuration in Fig. 3a is to drive the two partials together in the interface and subsequently to detach the lattice dislocation into the lower lamella. This then adopts the well-known non-planar core and is sessile.

3.2. Modelling of interactions between a lattice screw $\langle 101 \rangle$ superdislocation and 60° , 120° and 180° γ/γ -interfaces

The $\langle 101 \rangle$ superdislocation in single-phase γ -TiAl has two alternative core configurations [28,29]. The first one is planar and corresponds to splitting into three partials according to the reaction:



with a SISF and CSF on (111) planes. The second is non-planar and corresponds to the splitting into three partials according to the reaction:



with ribbons of SISF on (111) and $(\bar{1}\bar{1}1)$ planes. The former core structure is glissile with significantly lower Peierls stress than that of ordinary dislocations and moves at relatively low applied stresses. The latter is sessile but is favoured when the energy of the SISF is below a critical value. In violation of Schmid's law, the ability of the dislocation in its planar core configurations to glide depends strongly on the sense of shearing. The planar cores transform into a non-planar core structure after some limited glide under the effect of externally applied shear stress such that the $\frac{1}{6}[11\bar{2}]$ partial bounding the SISF would be leading during glide. When stress is applied in reverse direction ($\frac{1}{6}[112]$ partial would be trailing) the entire glissile core configuration retains its planar character and gradually moves onto an adjacent (111) layer [28,29].

3.2.1. Static core structure

We examined the dislocation core geometries that the lattice produces close to lamellar boundaries starting with two groups of initial configurations. In the first case, the starting unrelaxed configuration corresponding to reaction (4) is parallel to the lamellar boundary. The

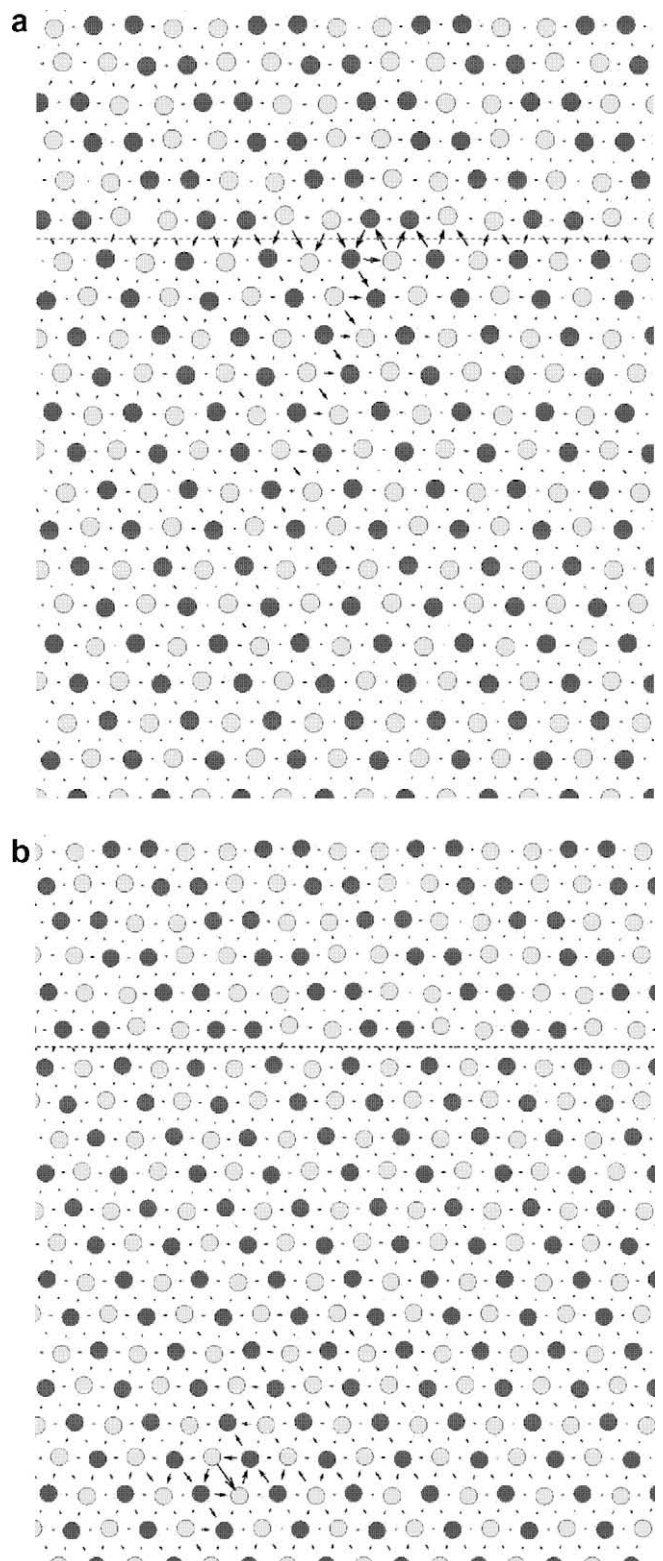


Fig. 3. Detachment of interfacial $\frac{1}{2}\langle 110 \rangle$ screw ordinary dislocation from the 60° γ/γ -lamellar boundary as a result of applied shear stress inducing glide force in a direction perpendicular to the lamellar boundary. (a) The core structure at a stress of $0.03C_{44}$. (b) The core structure at a stress of $0.035C_{44}$.

second group includes simulations of the planar core configuration situated on the cross-slip $(\bar{1}\bar{1}1)$ plane

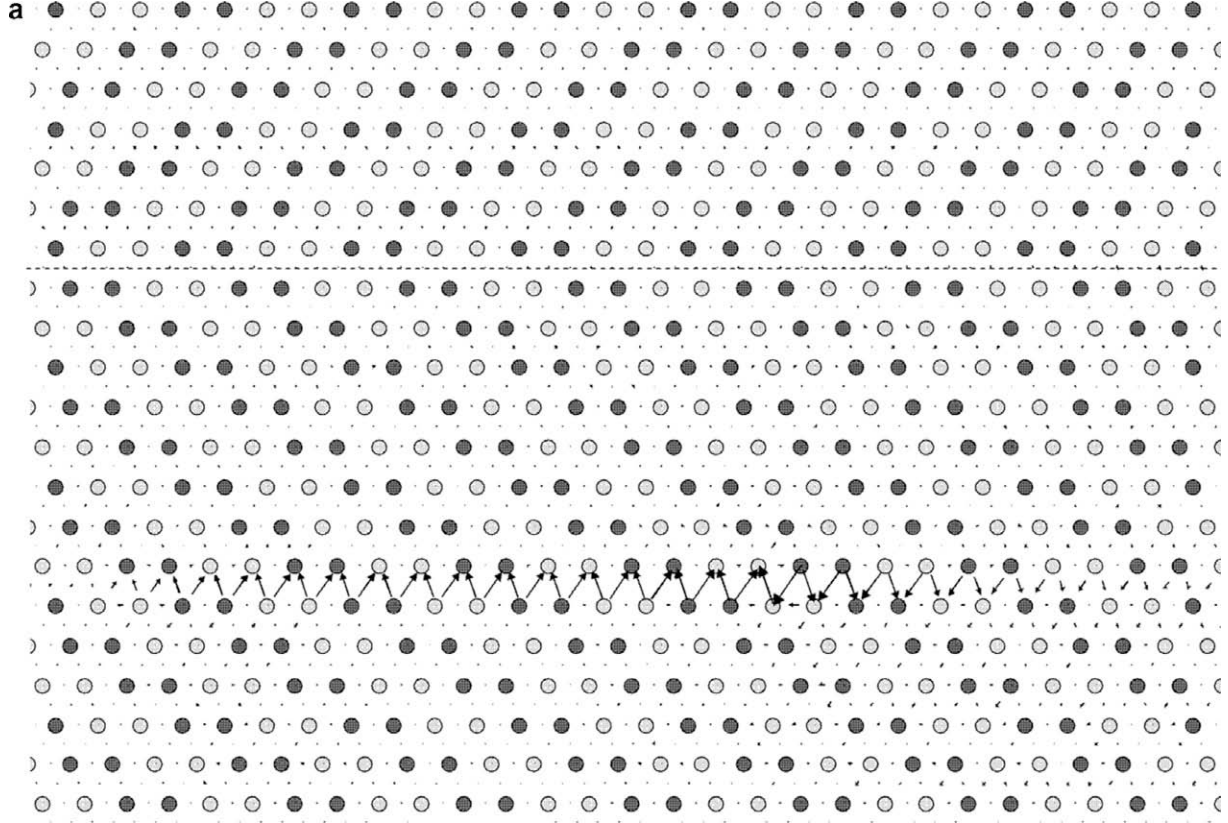
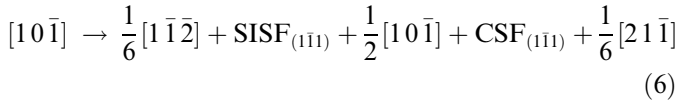


Fig. 4. Differential displacement maps of planar splittings of a $[10\bar{1}]$ screw superdislocation close to the $180^\circ \gamma/\gamma$ -lamellar boundary. (a) Core structure in $(1\bar{1}1)$ parallel to the lamellar boundary. (b) Core structure in a plane inclined at 180° to the γ/γ -lamellar boundary with $\frac{1}{6}[21\bar{1}]$ partial closer to the interface. (c) Core structure in a plane inclined to the lamellar boundary with $\frac{1}{6}[1\bar{1}\bar{2}]$ partial closer to the interface.

inclined with the lamellar interface. In this case, the ribbons of SISF and CSF are localized into the $(1\bar{1}1)$ plane and the starting unrelaxed planar configuration corresponds to the reaction:



3.2.1.1. $180^\circ \gamma/\gamma$ -interface. The relaxed core structure of the planar configuration (4) parallel to the $180^\circ \gamma/\gamma$ -interface is shown in Fig. 4a. The dislocation core retains the same structure. This configuration contains a narrow ribbon of CSF on the $(1\bar{1}1)$ plane on the right-hand side and a much wider ribbon of the SISF on the left-hand side. In the case where splitting according to the reaction (6) into the $(1\bar{1}1)$ plane inclined with the lamellar boundary was used as the initial configuration, the dislocation core also retains the same planar structure. We examined the core starting with two initial configurations—one with the $\frac{1}{6}[1\bar{1}\bar{2}]$ partial closer to the lamellar interface (Fig. 4b) and the other with $\frac{1}{6}[21\bar{1}]$ closer to the boundary (Fig. 4c). The results of the present atomistic simulations indicate that the planar core configurations of the superdislocation located in both $(1\bar{1}1)$ and $(1\bar{1}1)$ planes retain their glissile structure in proximity to the $180^\circ \gamma/\gamma$ -interface.

3.2.1.2. 60° and $120^\circ \gamma/\gamma$ -interfaces. A different situation arises when the same planar core structures are relaxed in the vicinity of 60° and 120° lamellar boundaries. In all cases, the initial planar core transforms into a non-planar sessile core configuration (5), which corresponds to the splitting of three partials with ribbons of SISF into $(1\bar{1}1)$ and $(1\bar{1}1)$ planes (Fig. 5). The results of the simulations indicate that the transformation of the core structure of the superdislocation is due to the elastic interactions between the dislocations and the lamellar boundaries.

In spite of strain accommodation by the misfit interfacial dislocations, a significant misfit seems to remain at the 60° and $120^\circ \gamma/\gamma$ -interfaces resulting in high coherency stresses. Even neglecting the non-ideality of the c/a ratio in our calculations, the coherency stresses arise due to the layout of atomic species changing as a result of the rotation that creates the lamellar boundary. We used atomistic stress tensor calculations [32] to determine the state of stress at the vicinity of the γ/γ -lamellar boundaries. The magnitude of the coherency stresses has been estimated in terms of the average local atomistic stresses. The results for the magnitudes of the shear stresses calculated close to all three kinds of γ/γ -interfaces are shown on Table 1. The magnitude of the average coherency shear stress estimated experimentally is 140 MPa [33].

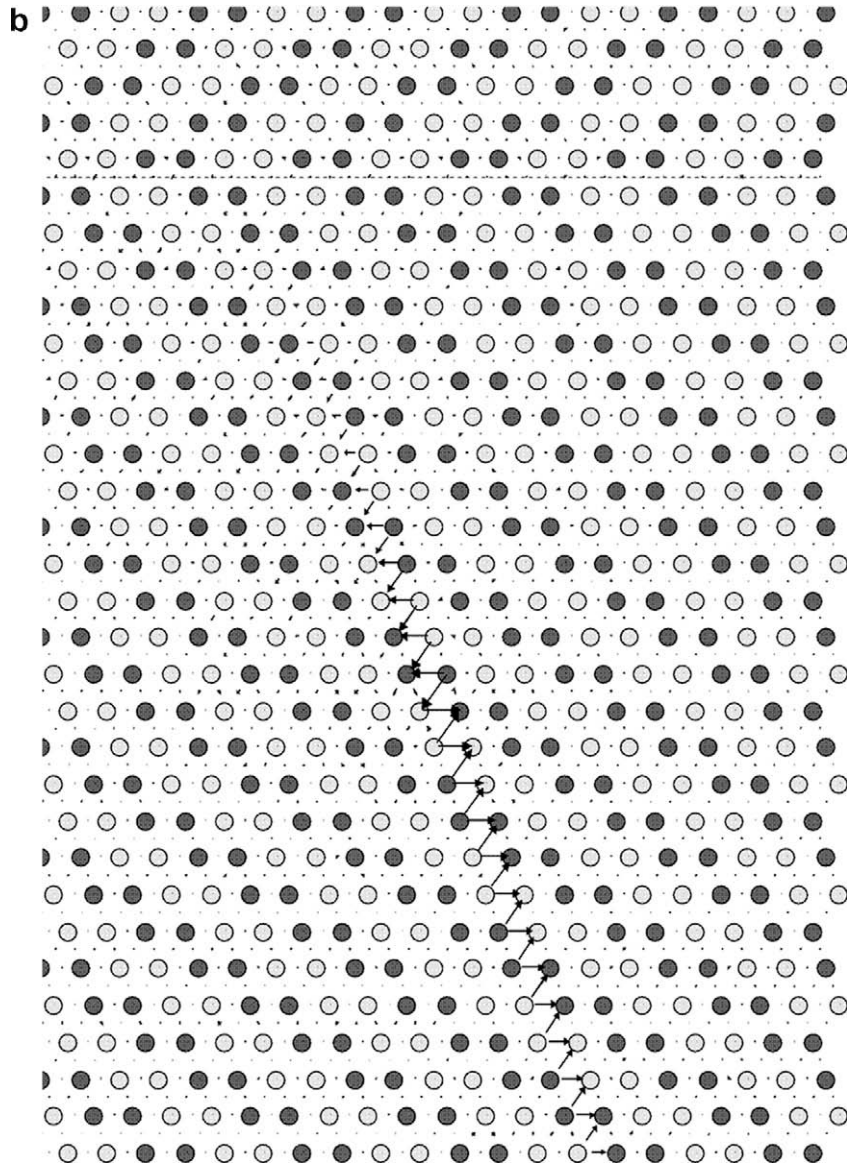


Fig. 4 (continued)

Coherency stresses, apart from exerting direct glide [34] and non-glide forces [35] on dislocations, can also modify the stacking-fault energies of the individual lamellae. An increase in the energy of CSF close to γ/γ -interfaces could make the planar core unstable and assist transformation to a non-planar core structure. Our atomistic simulations indicate that this mechanism could promote the formation of a non-planar core close to the $120^\circ \gamma/\gamma$ -interface due to the increase in the CSF energy (490 mJ m^{-2}) induced by coherency stress. These stresses do not substantially change the CSF energy close to the other two kinds of γ/γ -interface.

In our atomistic simulations, we also observe distortions of the non-planar $\langle 101 \rangle$ superdislocation core structure at the vicinity of 60° and $120^\circ \gamma/\gamma$ -interfaces, which could be attributed to the combined action of coherency stresses and elastic constant mismatch introducing glide forces on the

partial dislocations. The induced glide forces push the partial dislocations forming the non-planar core structure either in the octahedral planes of the SISFs, changing their width (Fig. 5a and b), or off the planes of the faults (Fig. 5c and d). The non-planar core is more distorted (Fig. 5c) and the SISF in the cross-slip plane is wider (Fig. 5a) close to the $120^\circ \gamma/\gamma$ -interface, where the higher magnitude of coherency stresses induce larger glide forces on the partial dislocations.

3.2.2. Effects of applied stress on core of glissile screw $\langle 101 \rangle$ superdislocation in proximity to the $180^\circ \gamma/\gamma$ -interface

3.2.2.1. Stress generating glide force in the direction parallel to the interface. The glide of the planar $\langle 101 \rangle$ superdislocation configuration in the direction parallel to the $180^\circ \gamma/\gamma$ -interface is similar to the glide of the same core structure in

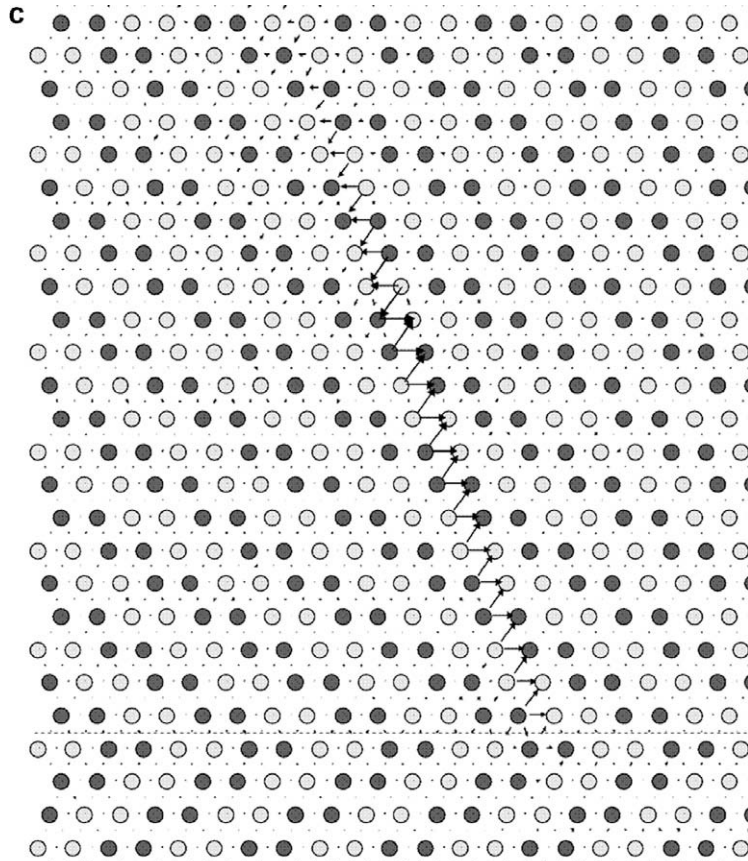


Fig. 4 (continued)

single-crystal L1₀ TiAl [28,29]. The planar cores transform into a non-planar core structure under the effect of externally applied shear stress such that the $\frac{1}{6}[1\bar{1}\bar{2}]$ partial bounding the SISF would be leading during glide. Under the effect of externally applied shear stress such that the $\frac{1}{6}[1\bar{1}\bar{2}]$ partial would be trailing during glide, the dislocation starts to move on the (111) plane at a stress of 0.01C₄₄. The leading CSF moves on an adjacent (111) layer. This configuration is planar, though with the CSF in an adjacent parallel plane to that of the unstressed state. Upon increasing the applied shear stress, the ribbon of SISF on the initial glide plane also starts to transform into an SISF in the adjacent parallel plane. In this way, the entire glissile core configuration gradually moves onto an adjacent (111) layer [29]. The results of our atomistic simulations indicate that the presence of the 180° γ/γ -interface does not change substantially the glide of the planar core configurations parallel to the lamellar boundary.

3.2.2.2. Stress generating glide force in the direction perpendicular to the lamellar boundary. A series of calculations at various applied strains was used to determine the glide of the planar core configuration (6) with ribbons of SISF and CSF on (111) in the direction of a 180° lamellar boundary. The shear stress was applied in the [101] direction in such a way that the dislocations were set to glide on

the (111) plane. We again examined the glide starting with two initial core configurations—one with the $\frac{1}{6}[1\bar{1}\bar{2}]$ partial closer to the lamellar interface and the other with $\frac{1}{6}[21\bar{1}]$ closer.

When applying the shear stress such that the $\frac{1}{6}[21\bar{1}]$ partial bounding the CSF would be leading during glide (Fig. 4b), the dislocation configuration starts to move on the (111) plane in direction of the lamellar boundary at a stress of 0.015C₄₄. The lamellar boundary blocks the dislocation after the leading $\frac{1}{6}[21\bar{1}]$ partial reaches the interface. At a stress of 0.045C₄₄, the leading CSF on the (111) plane transforms into a CSF on the (111) layer adjacent to the lamellar boundary (Fig. 6a). The CSF extends in the adjacent layer instead of the plane of lamellar boundary, presumably due to the higher energy of the CSF (550 mJ m⁻²) at the 180° γ/γ -interface than in bulk TiAl. With increasing applied shear stress, the ribbon of SISF on (111) also starts to transform into SISF in the same (111) plane parallel to the lamellar interface (Fig. 6b). Presumably, at high enough applied stress the entire planar configuration on the (111) plane will transform into a {101} dislocation with a planar core corresponding to splitting of three partials with SISF and CSF according to reaction (4) in a plane parallel to the 180° lamellar boundary. However, large-scale and lengthy atomistic calculations, which are beyond current capabilities, are

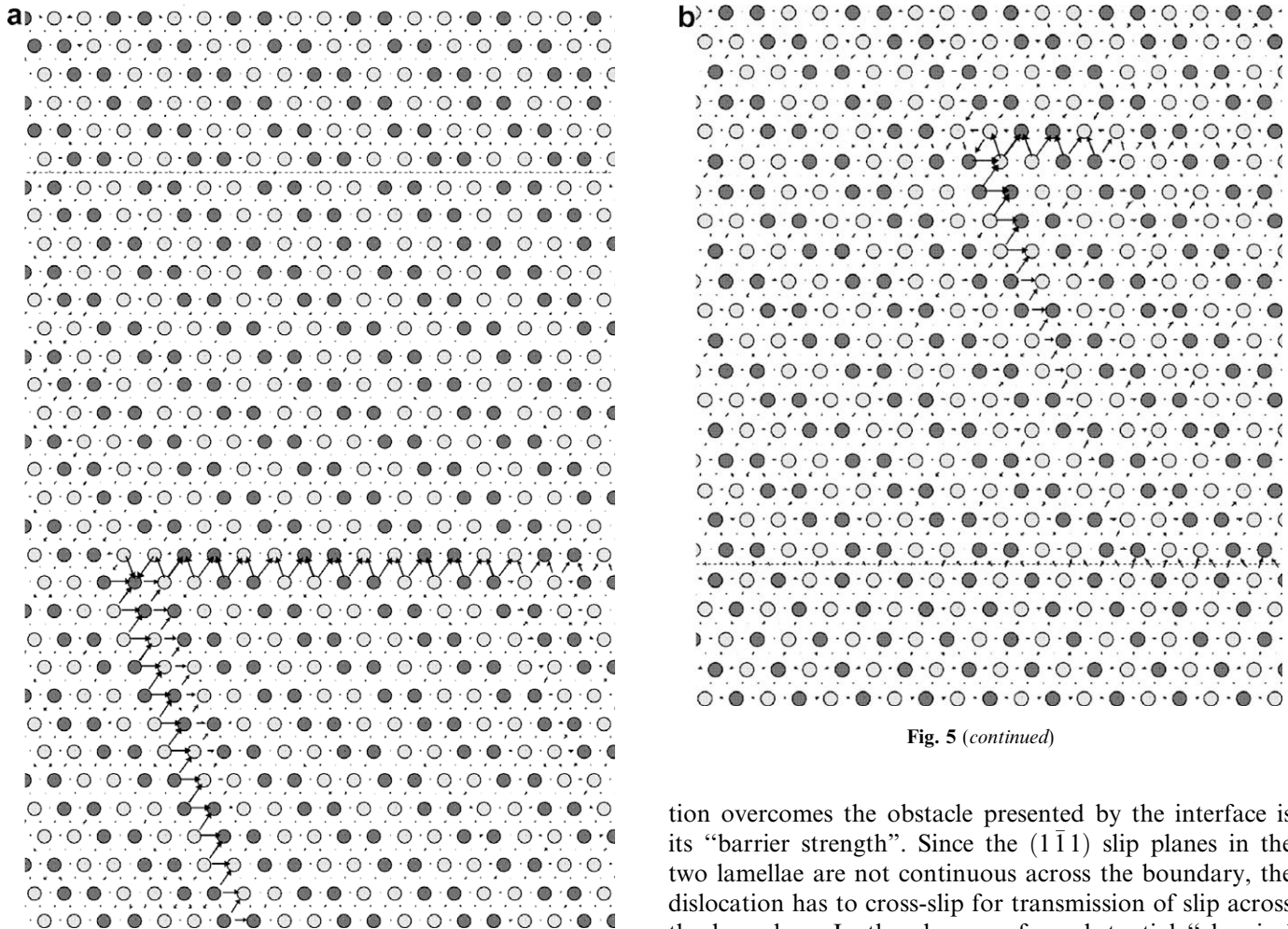


Fig. 5. Differential displacement maps of the planar splitting of $[10\bar{1}]$ screw superdislocation in planes inclined and parallel to the 60° and 120° γ/γ -lamellar boundaries. (a) Core structure in a plane inclined to the 120° γ/γ -lamellar boundary and with $\frac{1}{6}[2\bar{1}\bar{1}]$ partial closer to the interface. (b) Core structure in a plane inclined to the 60° γ/γ -lamellar boundary and with $\frac{1}{6}[1\bar{1}2]$ partial closer to the interface. (c) Core structure in a plane parallel to the 120° γ/γ -lamellar boundary; the $\frac{1}{6}\langle 112 \rangle$ partial bounding the SISF moves in the direction away from the lamellar boundary to extend the stacking fault on the secondary plane. (d) Core structure in a plane parallel to the 60° γ/γ -lamellar boundary; the $\frac{1}{6}\langle 112 \rangle$ partial bounding the SISF moves towards the lamellar boundary to extend the stacking fault on the secondary plane.

necessary for simulation of this process. However, we do not expect to observe transfer of slip across the 180° γ/γ -interface in this case.

In contrast, when the shear stress was applied such that the $\frac{1}{6}[2\bar{1}\bar{1}]$ partial would be trailing during glide (Fig. 4c), the dislocation is transmitted across the lamellar boundary. At an applied stress of $0.015C_{44}$, the leading $\frac{1}{6}[1\bar{1}2]$ partial overcomes the interface and moves into the adjacent lamella, leaving a ribbon of SISF behind it (Fig. 7a). At a stress of $0.034C_{44}$, the $\frac{1}{2}[10\bar{1}]$ lattice dislocation also penetrates into the second crystal (Fig. 7b). The entire planar configuration (6) moves into the adjacent lamella at an applied stress of $0.038C_{44}$. The stress at which a dislo-

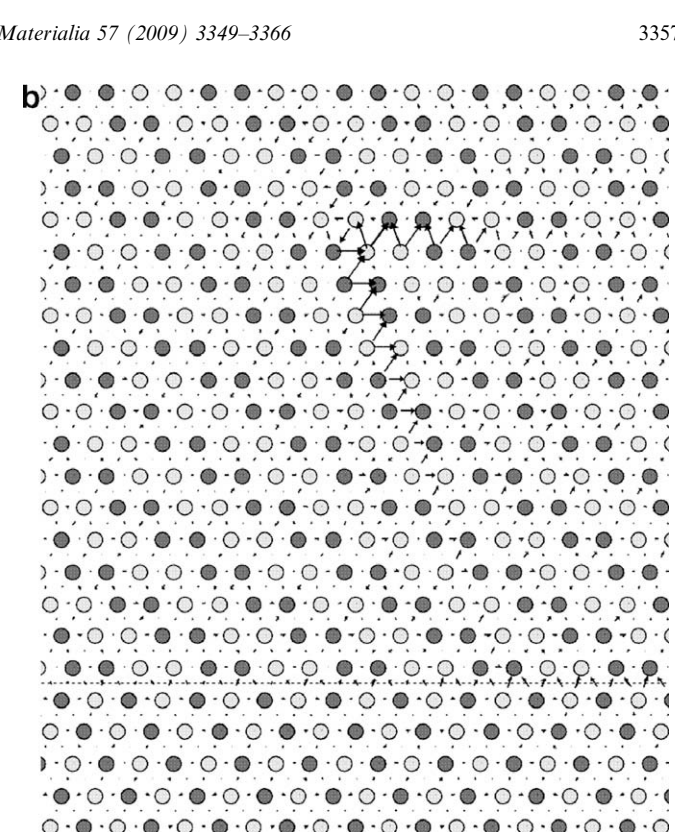


Fig. 5 (continued)

tion overcomes the obstacle presented by the interface is its “barrier strength”. Since the $(1\bar{1}1)$ slip planes in the two lamellae are not continuous across the boundary, the dislocation has to cross-slip for transmission of slip across the boundary. In the absence of a substantial “chemical effect” (stacking-fault energy change at the interface) [12] and elastic interactions, the blocking strength of the 180° lamellar boundary to the glide of superdislocations is due to the discontinuity of the slip planes across the interface.

3.2.3. Modelling of the interfacial $\langle 101 \rangle$ screw superdislocation

In order to study the interfacial $\langle 101 \rangle$ screw superdislocation in its planar core configuration, we used the splitting according to the reaction (4) as an initial configuration within the lamellar boundary plane. The resulting relaxed core structures retain the same planar character for all three kinds of γ/γ -interfaces (Fig. 8). When applying shear stress generating glide force parallel to the 180° lamellar boundary, such that the $\frac{1}{6}[2\bar{1}\bar{1}]$ partial bounding the CSF would be leading during glide, the dislocations start to move at a stress of $0.003C_{44}$. The superdislocation retains its planar core structure during glide in this direction. The Peierls stress for superdislocation glide in the lamellar boundary plane is considerably smaller than the CRSS for glide of the same dislocation in single-crystal L₁₀-TiAl, where it starts to move on the (111) plane at a stress of $0.01C_{44}$ [29]. Under the effect of externally applied shear stress such that the $\frac{1}{6}[11\bar{2}]$ partial would be leading during glide, the dislocation starts to move on the plane of the

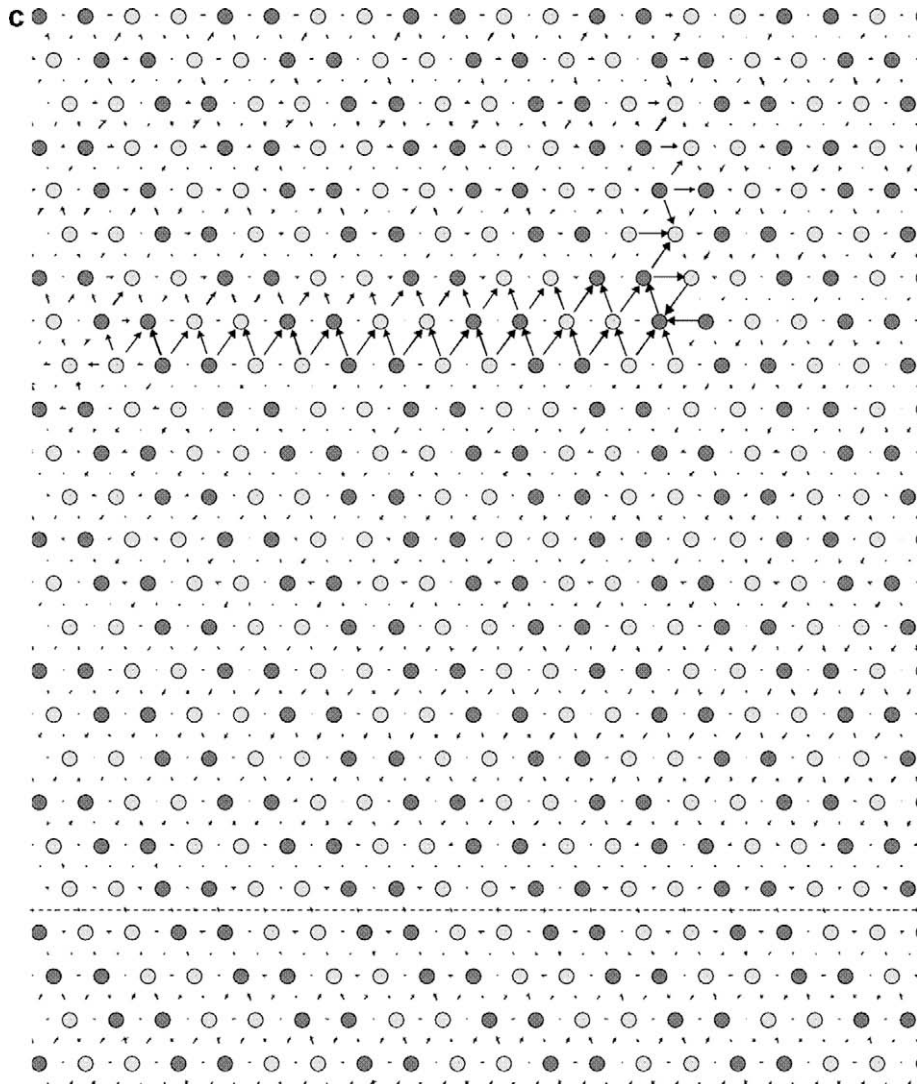


Fig. 5 (continued)

180° lamellar boundary at a stress of $0.013C_{44}$. The planar core of a lattice superdislocation transforms into non-planar core in single-crystal L1₀-TiAl when the stress is applied in the same direction. In contrast, the interfacial superdislocation retains its planar core structure when $\frac{1}{6}[1\bar{1}2]$ partial is leading during glide due to the discontinuity of the cross-slip plane at the lamellar boundary. We observed similar behaviour of the interfacial superdislocation in its planar core configuration in the 60° and 120° lamellar boundary planes.

Under applied shear stress generating glide force perpendicular to the 180° lamellar boundary, the planar core of the dissociated [10 $\bar{1}$] screw dislocation transforms to a non-planar sessile structure spreading into the lamellar interface and an intersecting plane in the upper lamellae (Fig. 9a). The non-planar core structure corresponds to dissociation into three partial dislocations separated by a CSF in the plane of the lamellar boundary and SISF extended in the γ -lamella. The SISF propagates in the γ -lamella as

result of the glide of $\frac{1}{6}\langle 112 \rangle$ twinning partial dislocations into a (111) plane inclined with the lamellar boundary.

Under an applied shear stress of $0.077C_{44}$, generating glide force perpendicular to the 60° lamellar boundary, the interfacial planar configuration (Fig. 8b) transforms into a lattice $\frac{1}{2}[1\bar{1}0]$ screw dislocation propagating in the γ -lamella and an interfacial $\frac{1}{2}[1\bar{1}0]$ ordinary dislocation remaining in the plane of the lamellar boundary (Fig. 9b). Both dislocations repel each other due to the elastic interaction between them. The core structure of the lattice dislocation is non-planar, spread into two (111) planes. The core of the interfacial ordinary dislocation is planar, corresponding to dissociation into two partials separated by CSF according to reaction (1). Upon increasing the applied stress, the interfacial dislocation could be expected to detach from the lamellar boundary and transform into a lattice $\frac{1}{2}[1\bar{1}0]$ screw dislocation in the γ -lamella according to the mechanism described in Section 3.1.2.2 (Fig. 3).

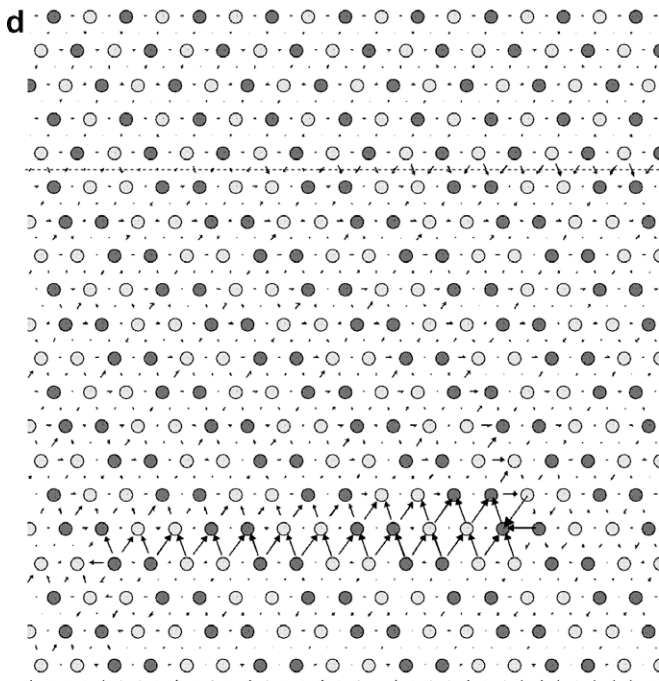


Fig. 5 (continued)

4. Discussion

It can be seen from our results that the lamellar structure in the two-phase material plays a pivotal role in the mechanical behaviour of polysynthetically twinned TiAl. The lamellar interfaces have previously been thought to play a double role [2]. One is to serve as major sources of dislocations and the other is to impede the movement of the dislocations. We now find that the lamellar boundaries modify the core structure and reduce the Peierls stress if a dislocation lies within the lamellar boundary plane. The interactions between dislocations and lamellar boundaries are usually regarded as a combination of elastic and atomistic effects. The former originate from the elastic anisotropy and misfit between the participating lamellae and long-range elastic fields of dislocations. The latter are associated with unique atomic structures of the lamellar boundaries, distinct properties of dislocation cores, and changes in dislocation Burgers vectors during the interaction. Owing to dramatic increases and decreases of planar fault energy within the lamellar boundaries, both the self-energy of the dislocations and the interaction energy between the Shockley partials continuously vary as the dislocations move toward the interface.

Table 1
Coherency stresses at the three γ/γ -interfaces. x , y and z directions are as defined in Section 2.

	60°	120°	180°
σ_{xy} (MPa)	21	99	0.1
σ_{xz} (MPa)	51	143	0.4
σ_{yz} (MPa)	45	172	0.7

Our results indicate that both ordinary and superdislocation slip can be activated inside the γ -lamellae. However, the confinement of the lamellar interfaces leads to highly anisotropic deformation behaviour. PST crystals exhibit a strong dependence of yield strength on the orientation angle between the lamellar boundaries and the load axes [2,4]. Two deformation modes for PST crystals of TiAl are reported in Ref. [4]: an easy mode, characterized by a glide parallel to the lamellar boundaries; and a hard mode, characterized by glide perpendicular to the interfaces. When the loading axis is parallel or perpendicular to the lamellar boundaries, the yield strength at room temperature is quite high, i.e. ~ 290 and 500 MPa [2,4]. In these configurations there is no resolved shear stress and therefore no driving force for slip on the (111) planes parallel to the lamellar boundaries. Slip must thus cross through the lamellar boundaries. In the γ -lamellae the deformation proceeds via normal slip on a set of inclined (111) planes. As a result the PST crystals loaded in the perpendicular orientation have a very high yield stress and often fracture at an elongation of about 20% without actually yielding. When the loading axis is inclined at around 45° to the lamellar boundaries, the sample can be easily deformed with yield strength ~ 90 MPa [2,4]. The deformation occurs in the easily deformable γ -lamellae via shearing along (111) planes parallel to the lamellar boundaries. After yielding starts, the sample deforms up to about 20% elongation and then fractures. The single-phase γ -TiAl fractures at room temperature before reaching 0.5–1% strain in tension, even if it has very low interstitial impurity levels. At room temperature the yield strength is ~ 250 MPa [36]. Like yield stress, the tensile elongation of PST crystals also depends strongly on the orientation angle. It is highest for the soft direction where the shear deformation is not impeded by the lamellar boundaries, and may easily exceed the maximum ductility of single-phase γ -TiAl material by a factor of more than 20. A detailed comparison of the mechanical properties of the materials with different microstructures can be found in a review by Appel and Wagner [2]. Two-phase γ -TiAl microstructures offering acceptable ductilities often show poor toughness, whereas microstructures with improved toughness have unsatisfactory ductility. This inverse correlation between tensile properties and resistance to fracture may be taken as an indication that the response of the two-phase TiAl to an applied load is controlled by a rather complex microstructure-dependent interplay between the micromechanisms of deformation and the mode of crack generation and propagation.

In agreement with experimental observation, the present atomistic simulation results predict reduction of the Peierls stress for both ordinary and superdislocations when they lie in the interfacial boundary of both 60° and 120° lamellar boundaries. Our atomistic simulations reveal that the $\frac{1}{2}\langle 110 \rangle$ screw dislocation splits into two partials separated by CSF according to reaction (1) within the 60° and 120° lamellar boundary planes. The reason for the dislocation core structure transformation as the

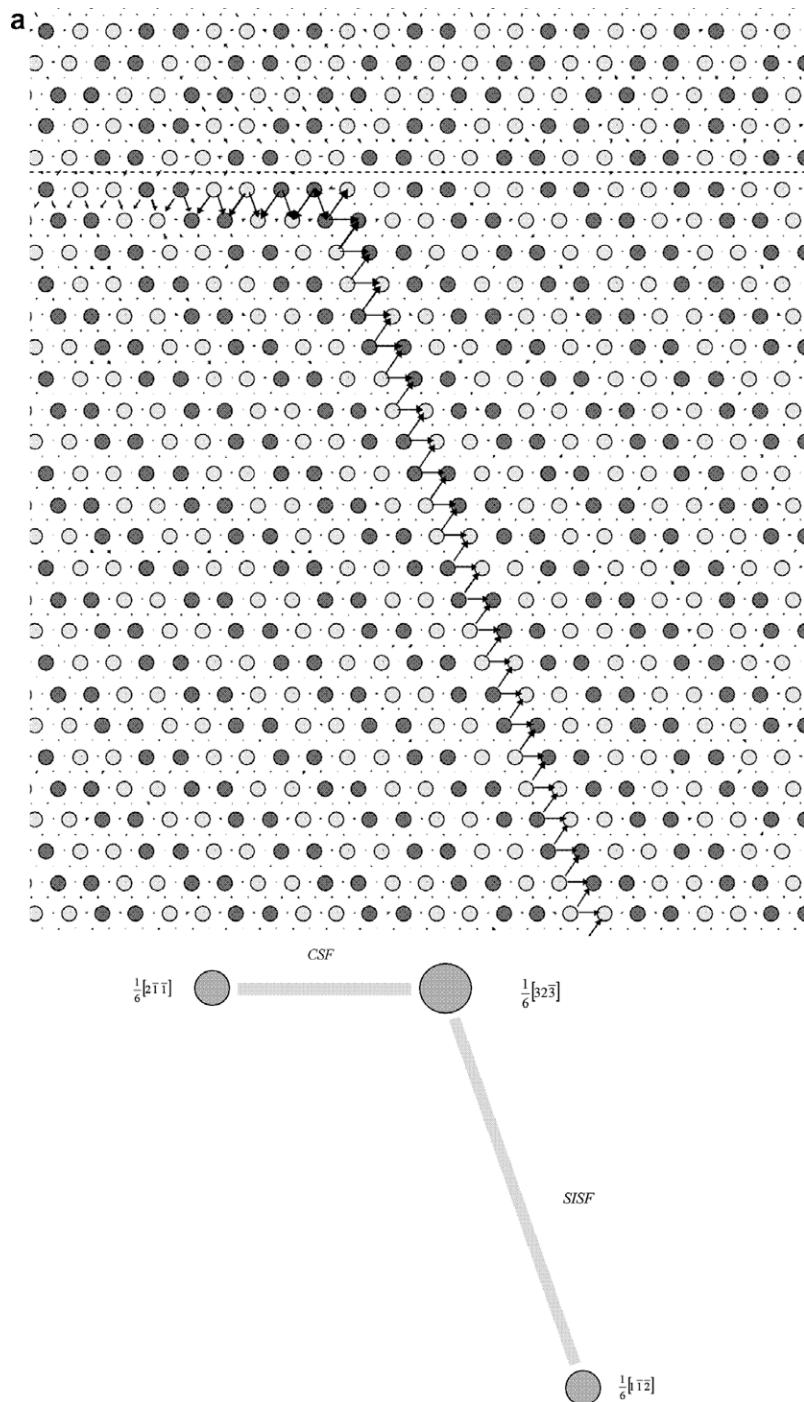


Fig. 6. Effect of applied shear stress inducing glide force in the direction perpendicular to the $180^\circ \gamma/\gamma$ -lamellar boundary on the planar splitting of $[10\bar{1}]$ screw superdislocation with $\frac{1}{6}[2\bar{1}\bar{1}]$ partial closer to the interface in a plane inclined to the lamellar boundary. (a) The core structure at a stress of $0.045C_{44}$. (b) The core structure at a stress of $0.058C_{44}$. Schematic pictures show corresponding dissociations.

dislocation moves from one lamella to the next is the stacking-fault energy change at the interface (“chemical” or “ γ -surface” mismatch). These dissociations take place because the energy of the CSF at the 60° and 120° lamellar boundaries is considerably smaller than the energy of the CSF in bulk TiAl. The non-planar core, which is typical for the ordinary dislocation in bulk $L1_0$ -TiAl, near and in the $180^\circ \gamma/\gamma$ -interfaces [18], transforms into a pla-

nar structure in and 1–2 atomic layers away from the 60° and 120° lamellar boundaries. While the presence of a 180° lamellar interface does not reduce the CRSS of the ordinary dislocation in the (111) plane, the planar core (1) is glissile and moves in the plane of the 60° and $120^\circ \gamma/\gamma$ -lamellar boundaries at applied stresses considerably smaller than the CRSS of ordinary and superdislocations in single-phase $L1_0$ -TiAl. The present results

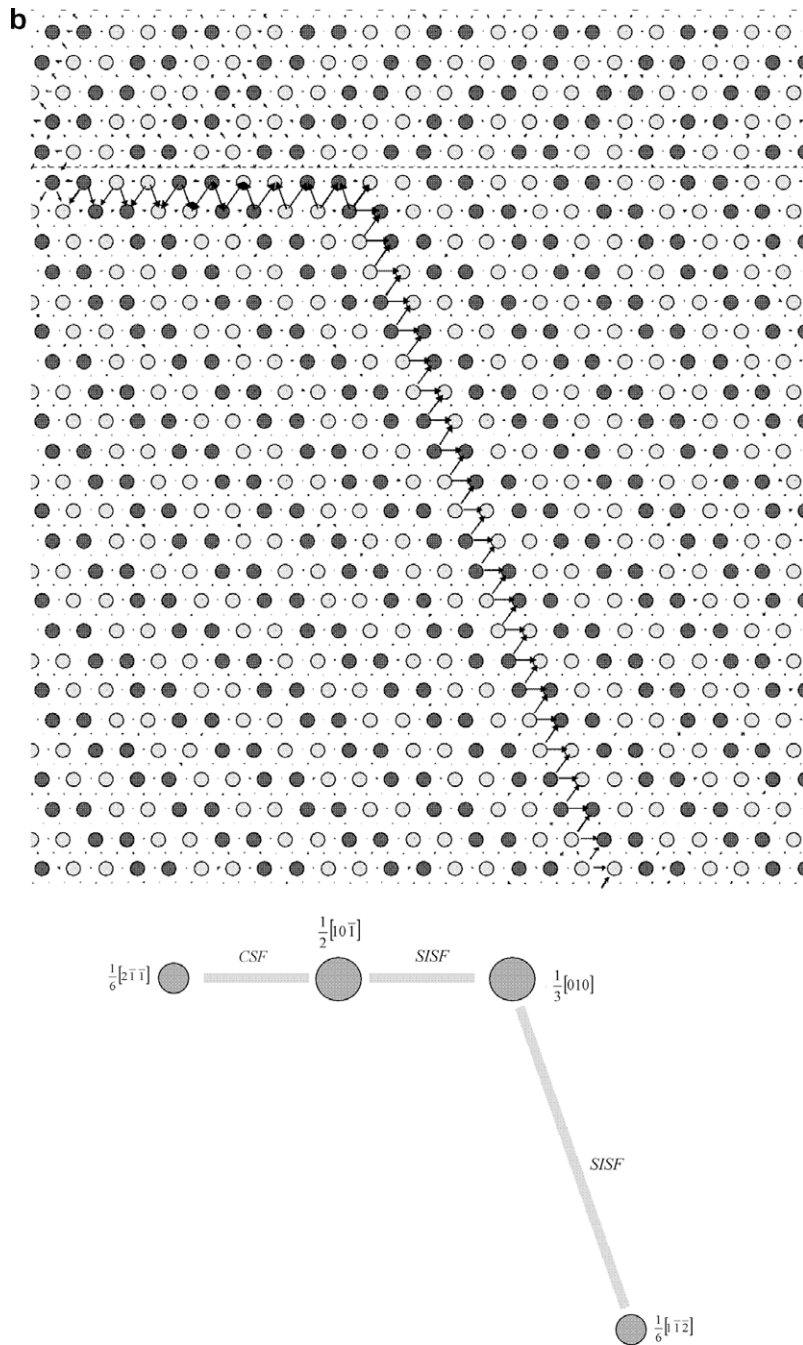


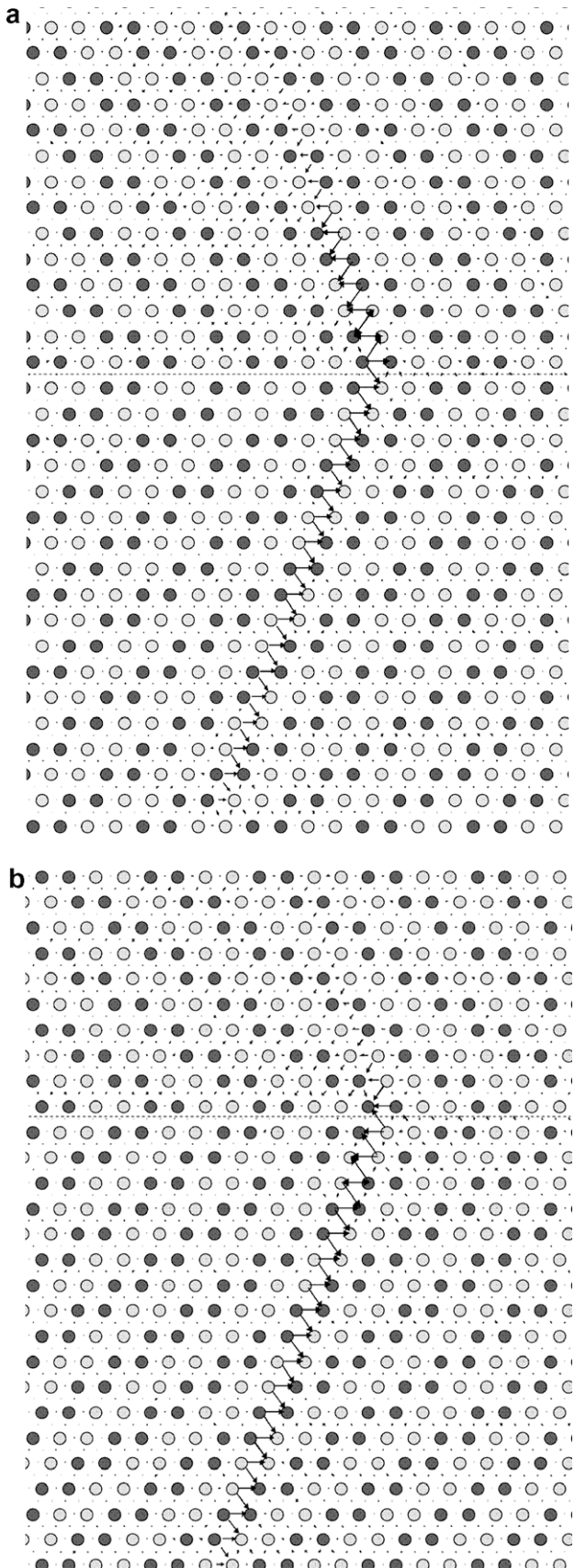
Fig. 6 (continued)

indicate that glide of interfacial ordinary dislocations along the 60° and 120° lamellar boundaries is the easiest slip mode in lamellar γ -TiAl. The Peierls stress for interfacial superdislocation glide is also considerably smaller than the CRSS for activation of superdislocation glide in single-crystal L₁₀-TiAl. The increased mobility of ordinary and superdislocations along the lamellar interfaces will facilitate plastic deformation in this direction.

Under applied shear stress generating glide forces towards the lamellar boundary, ordinary screw dislocations can glide through a 180° interface [18]. In the absence of

γ -surface interactions, the blocking strength of the 180° γ/γ -lamellar boundary to the glide of ordinary dislocations is due to the discontinuity of the slip planes across the interface. In contrast, ordinary dislocations can not be transmitted across the 60° and 120° lamellar boundaries. Instead, microtwins are formed as result of glide of $\frac{1}{6}(112)$ twinning partial dislocations into the $(1\bar{1}1)$ plane in the second lamella, leaving ribbons of SISF behind them. Under stress applied in the reverse direction (the glide force towards the first lamella) the interfacial planar configuration (1) detaches from the 60° and 120° lamellar

boundaries and transforms into a lattice $\frac{1}{2}[1\bar{1}0]$ screw dislocation in the first lamella. The critical stress required



to renucleate the partials depends on the difference between CSF energy in lamellar boundaries and in bulk γ -TiAl.

It can also be seen from our results that coherency stresses at the lamellar interfaces have strong effects on the deformation properties of polysynthetically twinned crystals. Our calculations indicate that significant misfit remains at the 60° and 120° γ/γ -interfaces in the regions of matching lattices between the misfit dislocations. The coherency stresses arise due to changes in the layout of atomic species a result of the rotation creating the lamellar boundary. The transformation of the planar core configurations into a non-planar form is principally controlled by the shear stress in the cross-slip plane. A sessile structure forms if the RSS on the cross-slip plane acts to drive the $\frac{1}{6}\langle 112 \rangle$ partial dislocation in a direction extending the SISF in this plane [28,29,36]. Interactions between elastic fields generated by the planar core structure of a superdislocation and the 60° and 120° γ/γ -lamellar boundaries assist transformation of the glissile core geometry of the $\langle 101 \rangle$ screw dislocation into a non-planar sessile core configuration. Coherency stresses induced by the lamellar interfaces produce glide forces that push the partial dislocations off the octahedral glide plane. In our atomistic simulations, the sense of shearing generated by the coherency stresses is such that RSS on the cross-slip plane always acts in a direction extending the SISF in this plane. In this way, coherency stresses promote the formation of sessile core configurations through cross-slip of the CSF in the primary glide plane, forming SISF located on the cross-slip plane. The preservation of the planar core structure in proximity to the 180° γ/γ -interface, where the coherency stresses are negligible compared to the stresses in vicinity of the 60° and 120° γ/γ -interfaces, indicates that the transformation of the planar core configuration into the non-planar form is primarily due to the coherency stress arising at the 60° and 120° lamellar boundaries. The modulus mismatch (the Koehler barrier) also introduces forces between a dislocation and its image in the interface [35]. Image forces assist or act against extension of SISF in the cross-slip plane, depending on whether the $\frac{1}{6}\langle 112 \rangle$ partial bounding the SISF would move towards the lamellar boundary (Fig. 5d) or in the reverse direction (Fig. 5c) to extend the stacking fault on the secondary plane. In both cases, however, we observe cross-slip of the CSF in the glide plane, forming SISF located on the secondary plane. Hence, transformations of the initial planar core into a non-planar sessile core configuration are primarily due to the coherency strains arising at the 60° and 120° lamellar boundaries. It is worth mentioning that the Yoo torque [37] (anisotropic interaction forces on dissociated screw dis-

Fig. 7. Effect of applied shear stress inducing glide force in the direction perpendicular to the 180° γ/γ -lamellar boundary on the planar splitting of $[101]$ screw superdislocation with $\frac{1}{6}[1\bar{1}2]$ partial closer to the interface in a plane inclined with the lamellar boundary. (a) The core structure at a stress of 0.015C₄₄. (b) The core structure at a stress of 0.034C₄₄.

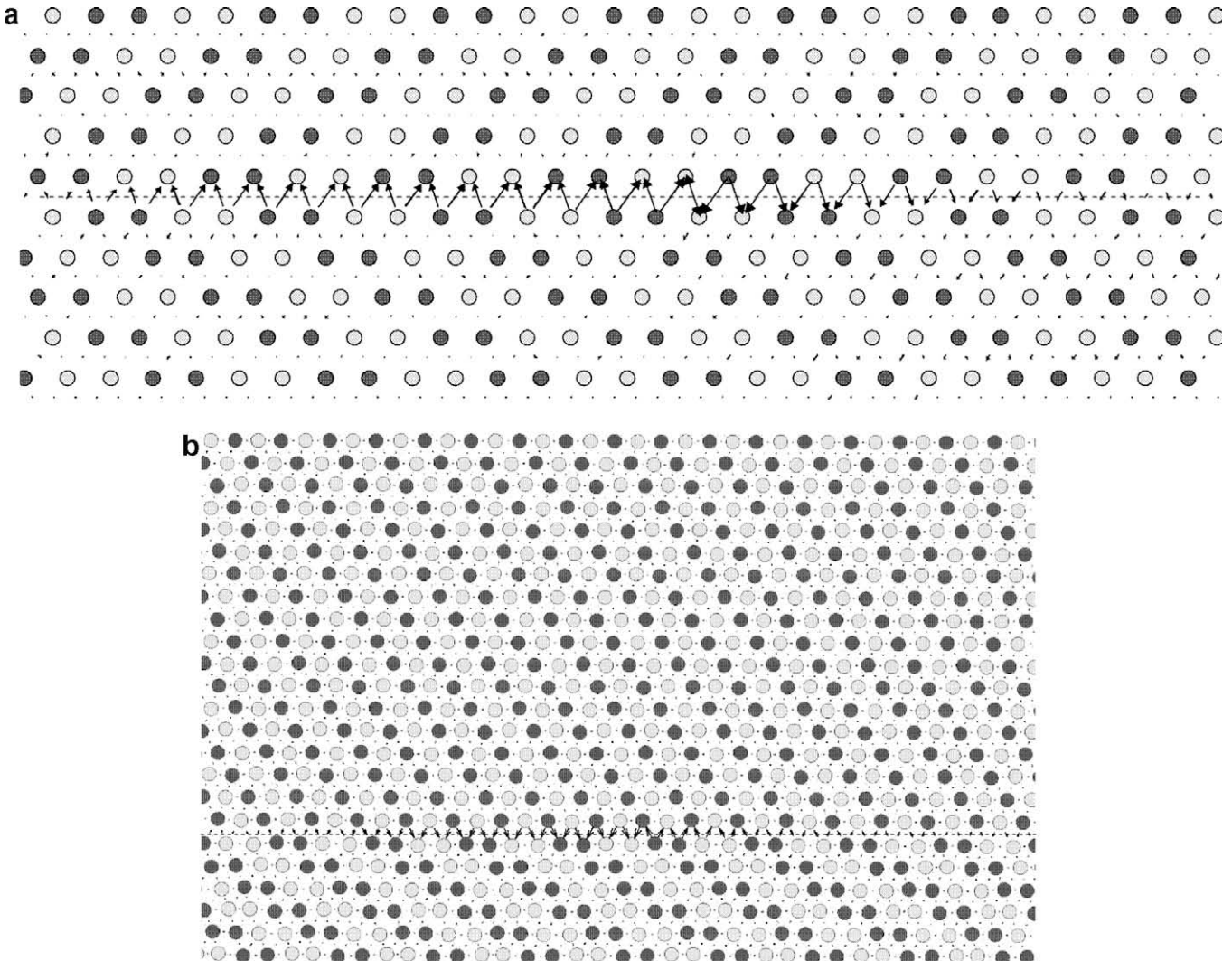


Fig. 8. Differential displacement maps of planar splittings of $[10\bar{1}]$ screw interfacial superdislocation. (a) Core structure in the $180^\circ \gamma/\gamma$ -lamellar boundary. (b) Core structure in the $60^\circ \gamma/\gamma$ -lamellar boundary.

locations) also promotes the formation of sessile core configuration [38]. The sessile structure forms close to 60° and $120^\circ \gamma/\gamma$ -lamellar boundaries since both RSS and the Yoo torque assist creation of the correct stacking fault on the cross-slip plane. Presumably, Escaig forces exerted by the coherency stresses on the edge components of the Shockley partials do not play a major role in the cross-slip locking of superdislocations in γ -TiAl. Results of analysis of the Escaig effect on the CSF separation of a pair of Shockley partial dislocations in γ -TiAl indicate that the applied stress has little or no effect on the magnitude of the CSF dissociation [39].

The ability of the superdislocation in its planar core configurations to glide depends strongly on the sense of shearing [28,29]. The glide of the planar splitting is found to be very different depending on whether the $\frac{1}{6}\langle 112 \rangle$ partial bounding the SISF is leading or trailing. In the latter case they remain glissile, while in the former case the glissile planar core transforms into a sessile one. In lamellar γ -TiAl, the 180° lamellar boundary blocks the planar config-

uration after the leading $\frac{1}{6}[21\bar{1}]$ partial reaches the interface. In this case, formation of a planar configuration with CSF on an adjacent parallel layer is hampered by the discontinuity of the slip planes across the interface. Instead, the leading partial cross-slips close to the interface under the action of the applied shear stress and the CSF on the primary $(1\bar{1}1)$ plane transforms into a CSF on a (111) layer parallel to the lamellar boundary (Fig. 6). Thus, no slip is transmitted across the $180^\circ \gamma/\gamma$ -interface in this case. The opposite situation arises when the shear stress is applied such that the $\frac{1}{6}(211)$ partial would be trailing during glide towards the $180^\circ \gamma/\gamma$ -interface (Fig. 7). The dislocation is transmitted across the lamellar boundary. However, the glissile planar core transforms into a sessile one in single-phase γ -TiAl when the $\frac{1}{6}\langle 112 \rangle$ partial would be leading during glide. This mechanism occurs after some limited glide [29]. The transformation takes place because in this case the RSS on the secondary cross-slip plane acts to extend the SISF in this plane. Hence, the majority of the glissile superdislocations will transform into sessile config-

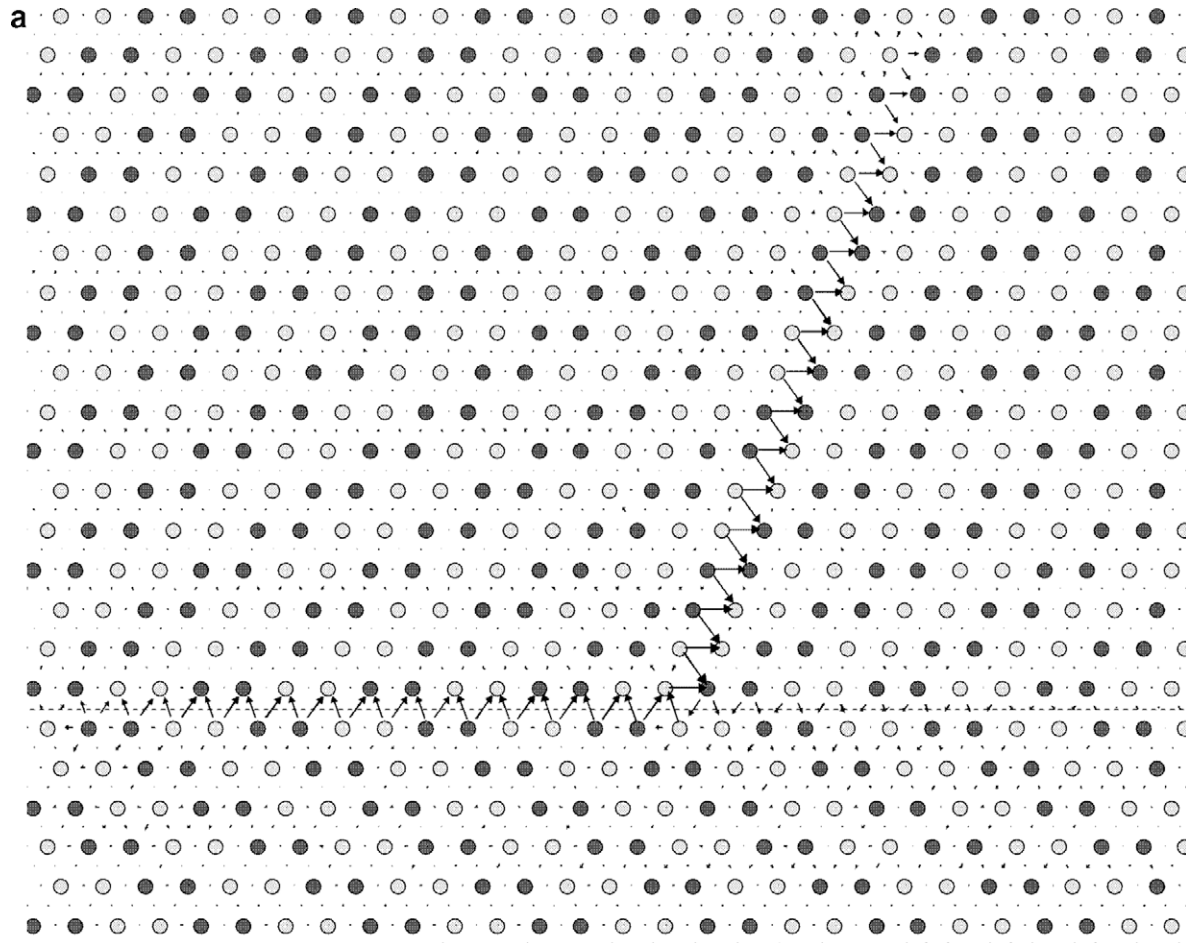


Fig. 9. Effect of applied shear stress inducing glide force perpendicular to the lamellar boundary on the planar splitting of $[10\bar{1}]$ interfacial screw superdislocation. (a) $180^\circ \gamma/\gamma$ -lamellar boundary. (b) $60^\circ \gamma/\gamma$ -lamellar boundary.

urations before reaching the lamellar boundary when the $\frac{1}{6}\langle 112 \rangle$ partial would be leading during glide. Only a limited number of these dislocations, situated close to the $180^\circ \gamma/\gamma$ -lamellar boundary, will reach the interface, and those that are transmitted through the lamellar boundary will be locked in the second lamella as a result of transformation of the glissile core into a non-planar sessile configuration. The glissile superdislocations thus become almost completely locked in proximity of the γ/γ -lamellar boundaries. The only active superdislocation slip mode inside a γ -lamellae close to the γ/γ -lamellar boundaries remains the glide of a planar core configuration in a plane parallel to the $180^\circ \gamma/\gamma$ -interface.

Following the results presented in previous sections we may speculate on the reasons for the different glide mechanisms of dislocations in bulk and lamellar TiAl. The lower density of mobile superdislocations in the lamellar microstructure can be interpreted through the effect of the interfaces. As a result of elastic interactions and atomistic effects (γ -surface interactions and discontinuity of glide planes across the lamellar boundaries) the planar glissile core geometry of the superdislocation transforms to a non-planar sessile core in lamellar TiAl close to the γ/γ -lamellar interfaces. The glissile superdislocations, moving on slip

planes parallel and inclined with the lamellar boundaries, thus became almost completely locked in proximity to the lamellar boundaries.

Activation of twinning at room temperature in lamellar TiAl can also be interpreted in terms of the effect of the lamellar boundaries. Our atomistic simulations suggest that under a number of circumstances SISFs are formed at the lamellar boundaries under applied shear stresses on interfacial ordinary or superdislocations and propagate in the γ -lamellae. These faults may serve as nuclei for twinning. Atomistic modelling of nucleation of twinning partial dipoles in the layer neighbouring the fault shows that the stress needed to nucleate a dipole adjacent to a SISF is appreciably lower than if single partials are considered [40]. A wider twin could be formed by extension of such dipoles in adjacent (111) planes. Thus, twinning could be expected to be an easier deformation mode at low temperature in lamellar TiAl than in single-crystal $L1_0$ -TiAl.

These mechanisms produce a lower activity of superdislocations and a higher activity of twinning in the lamellar structure than in the non-lamellar one. Furthermore, in the lamellar structure, ordinary dislocations cannot be transmitted across the 60° and 120° lamellar boundaries. The reduced activity of superdislocations on (111) planes inclined to the

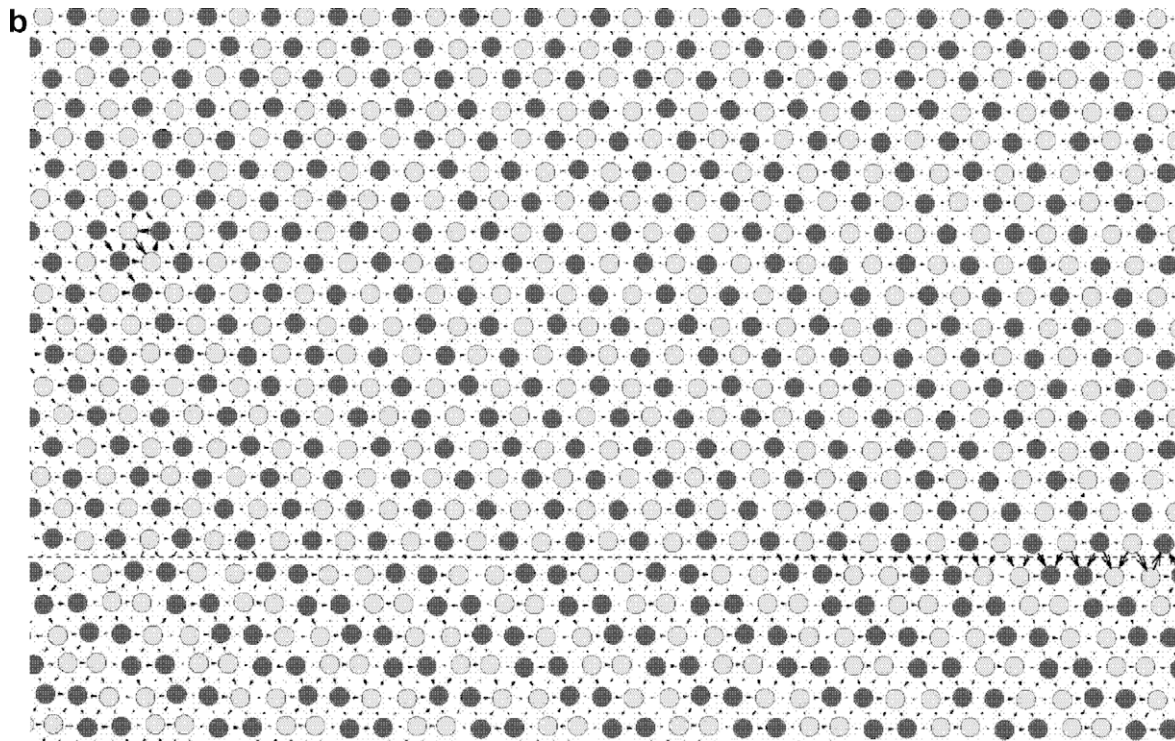


Fig. 9 (continued)

lamellar boundaries and the blocking strength of the γ/γ -lamellar interfaces to the glide of ordinary dislocations can explain the higher yield stress in PST when the loading axis is perpendicular to the lamellar boundaries.

The higher density of ordinary dislocations in the lamellar microstructure can also be interpreted in terms of the effect of the interfaces, where a very high density of ordinary interfacial dislocations is found [41]. Most probably, the reason for the high density of ordinary dislocations is the detachment of ordinary interfacial dislocations, accumulated at the lamellar boundaries, and their propagation into the interior of the lamellae. The decomposition of the interfacial $\langle 101 \rangle$ superdislocations into ordinary dislocations at the lamellar interface could also be one of the possible reasons for the experimentally observed higher density of ordinary dislocations in lamellar than in non-lamellar TiAl at low temperature. The transformation of a superdislocation into two ordinary dislocations at a lamellar interface is allowed for twin and other orientations, when the Burgers vector of the superdislocation is parallel to the interface.

5. Conclusions

Atomistic simulations of the interactions between the dominant lattice dislocations in γ -TiAl (screw $\frac{1}{2}\langle 110 \rangle$ ordinary and $\langle 101 \rangle$ superdislocations) with all three kinds of γ/γ -lamellar boundaries in PST TiAl have been made using a BOP for γ -TiAl. We studied the dislocation core geometries that the lattice produces in proximity to lamellar boundaries and the way in which these cores are affected by the elastic and atomistic effects of dislocation-lamellar

boundary interaction. We also studied the way in which the interfaces affect the activation of ordinary dislocation and superdislocation slip inside the γ lamellae and transfer of plastic deformation across lamellar boundaries.

In summary we believe that among the very complex behaviour of dislocations in PST γ -TiAl we have discovered three new phenomena in the plastic response of these materials at the atomic scale.

1. Two new roles for the γ/γ -interfaces emerge: (a) dramatic reduction of the Peierls stress for both ordinary and superdislocations when they lie in the interfacial boundary of both the 60° and 120° lamellar boundaries and (b) stabilization of the glissile, planar core of superdislocations within the 60° and 120° lamellar boundary planes as a consequence of greatly reduced CSF energy. Conversely, the CSF energy is increased with respect to bulk at the 180° lamellar boundary.
2. Transformation of superdislocations within the 60° and 120° lamellar boundaries and subsequent detachment of an ordinary dislocation which is released into the lamella.
3. Emission of a twinning dislocation following the blocking of an ordinary dislocation after gliding in the 60° and 120° lamellar boundary.

Acknowledgements

The authors wish to thank Prof. V. Vitek of the University of Pennsylvania for helpful discussions during the course of this work. This research was supported by the EPSRC, under Grant No. EP/E025854/1 and was also sup-

ported by a Grant from the HPC-Europa program of the European Council.

References

- [1] Kim YW. JOM 1989;41:24–30.
- [2] Appel F, Wagner R. Mater Sci Eng 1998;R22:187–268.
- [3] Yamaguchi M et al. In: Horton JA et al., editors. High-temperature intermetallic alloys VI, Part 1. Mat. res. soc. symp. proc., vol. 364. Pittsburgh, PA: Materials Research Society; 1995. p. 3–16.
- [4] Inui H, Oh MH, Nakamura A, Yamaguchi M. Philos Mag A 1992;66:539–56.
- [5] Yamaguchi M, Inui H, Yokoshima S, Kishida K, Johnson DR. Mater Sci Eng A 1996;213:25–31.
- [6] Christian JW, Laughlin DE. Acta Metall 1988;36:1617–42.
- [7] Sun YQ, Hazzledine PM, Christian JW. Philos Mag A 1993;68:471–94.
- [8] Inui H, Matsumuro M, Wu DH, Yamaguchi M. Philos Mag A 1997;75:395–424.
- [9] de Koning M, Kurtz RJ, Bulatov VV, Henager CH, Hoagland RG, Cai W, et al. J Nucl Mater 2003;323(2–3):281–9.
- [10] Jin ZH, Gumbsch P, Ma E, Albe K, Lu K, Hahn H, et al. Scripta Matell 2006;54(6):1163–8.
- [11] Jang H, Farkas D. Mater Lett 2007;61(3):868–71.
- [12] Rao SI, Hazzledine PM. Philos Mag A 2000;80(9):2011–40.
- [13] Hoagland RG, Kurtz RJ, Henager CH. Scripta Matell 2004;50(6):775–9.
- [14] Henager CH, Kurtz RJ, Hoagland RG. Philos Mag 2004;84(22):2277–303.
- [15] Hasnaoui A, Derlet PM, Van Swygenhoven H. Acta Matell 2004;52(8):2251–8.
- [16] Van Swygenhoven H, Derlet PM, Hasnaoui A. Phys Rev B 2002;66(2):24101.
- [17] Spearot DE, Jacob KI, McDowell DL. Acta Matell 2005;53(13):3579–89.
- [18] Katzarov IH, Cawkwell MJ, Paxton AT, Finnis MW. Philos Mag 2007;87:1795–810.
- [19] Pettifor DG. Phys Rev Lett 1989;63:2480–3.
- [20] Znam S, Nguyen-Manh D, Pettifor DG, Vitek V. Philos Mag A 2003;83:415–38.
- [21] Znam S. PhD thesis, University of Pennsylvania; 2001.
- [22] Pettifor DG, Aoki M. Philos Trans Roy Soc London Ser A – Math Phys Eng Sci 1991;334:439–49.
- [23] Skinner AJ, Pettifor DG. J Phys: Condens Matter 1991;3:2029–47.
- [24] Nguyen-Manh D, Pettifor DG, Znam S, Vitek V. In: Turchi PEA, Gonis A, Colombo L, editors. Tight-binding approach to computational materials science, vol. 491. Pittsburgh, PA: Materials Research Society; 1998. p. 353–8.
- [25] Woodward C, Rao SI. Philos Mag A 2004;84:401–13.
- [26] Vitek V, Ito K, Siegl R, Znam S. Mater Sci Eng A 1997;240:752–60.
- [27] Ehmann J, Fähnle M. Philos Mag A 1998;77:701–14.
- [28] Porizek R, Znam S, Nguyen-Manh D, Vitek V, Pettifor DG. In: Mat. res. soc. symp. proc., vol. 753; 2003. p. BB4.3.1–6.
- [29] Katzarov IH, Paxton AT. Philos Mag, submitted for publication.
- [30] Hazzledine PM, Kad BK. Mater Sci Eng A 1995;192/193:340–6.
- [31] Fu CL, Yoo MH. Scripta Matell 1997;37:1453–9.
- [32] Born M, Huang K. Dynamical theory of crystal lattices. Oxford: Clarendon Press; 1954.
- [33] Hazzledine PM, Kad BK, Fraser HL, Dimiduk DM. In: MRS symp., vol. 273; 1992. p. 81–6.
- [34] Sutton AP, Baluffi RW. Interfaces in crystalline materials. Oxford: Clarendon Press; 1995.
- [35] Escaig B. In: Rosenfield AR, Hahn GT, Bement AL, Jafee RI, editors. Proceedings of the Battelle colloquium dislocation dynamics. New York: McGraw Hill; 1968. p. 655.
- [36] Zupan M, Hemker KJ. Acta Matell 2003;51:6277–90.
- [37] Yoo MH. Acta Metall 1987;35:1559–69.
- [38] Yoo MH, Fu CL. Metall Mater Trans A 1998;29:49–63.
- [39] Paidar V, Pope DP, Vitek V. Acta Metall 1984;32:435–48.
- [40] Nomura M, Kim Min-Chul, Vitek V, Pope DP. In: Kim YW, Dimiduk DM, Loretto MH, editors. Gamma titanium aluminides. Warrendale, PA: TMS; 1999. p. 67–73.
- [41] Parrini L. J Alloys Compd 1998;270:203–11.
- [42] Vitek V, Rerrin RC, Bowen DK. Philos Mag A 1970;21:1049–74.